Rapid Discovery of Self-Assembling Peptides with One-Bead One-Compound Peptide Libraries

Peipei Yang
National Center for Nanoscience and Technology

Yi-Jing Li
CAS Center for Excellence in Nanoscience, CAS Key Laboratory for Biomedical Effects of Nanomaterials and Nanosafety, National Center for Nanoscience and Technology

Yan Cao
Institute for Advanced Study, Shenzhen University https://orcid.org/0000-0001-8897-8385

Lu Zhang
Department of Biochemistry and Molecular Medicine, UC Davis NCI-designated Comprehensive Cancer Center, University of California Davis https://orcid.org/0000-0002-7492-6047

Jia-Qi Wang
National Center for Nanoscience and Technology

Zi-Wei Lai
Institute for Advanced Study, Shenzhen University

Kuo Zhang
National Center for Nanoscience and Technology https://orcid.org/0000-0003-3687-3172

Wenwu Xiao
Department of Biochemistry and Molecular Medicine, UC Davis NCI-designated Comprehensive Cancer Center, University of California Davis

Hui Cao
Department of Materials Physics and Chemistry, School of Materials Science and Engineering, University of Science and Technology Beijing

Lei Wang
National Center for Nanoscience and Technology https://orcid.org/0000-0003-1405-9815

Hao Wang
National Center for Nanoscience and Technology

Ruiwu Liu
University of California Davis

Kit Lam (kslam@ucdavis.edu)
Department of Biochemistry and Molecular Medicine, UC Davis NCI-designated Comprehensive Cancer Center, University of California Davis https://orcid.org/0000-0002-3076-6969

Article

Keywords: Self-assembly, OBOC, Peptide, Screening, Nanomaterials

Posted Date: November 30th, 2020

DOI: https://doi.org/10.21203/rs.3.rs-109949/v1

Version of Record: A version of this preprint was published at Nature Communications on July 23rd, 2021. See the published version at https://doi.org/10.1038/s41467-021-24597-5.

Abstract

Self-assembling peptides have shown tremendous potential in the fields of material sciences, nanoscience, and medicine. Because of the vast combinatorial space of even short peptides, identification of self-assembling sequences remains a challenge. Herein, we develop an experimental method to rapidly screen a huge array of peptide sequences for self-assembling property, using the one-bead one-compound (OBOC) combinatorial library method. In this approach, peptides on beads are N-terminally capped with nitro-1,2,3-benzoxadiazole, a hydrophobicity-sensitive fluorescence molecule. Beads displaying self-assembling peptides would fluoresce under aqueous environment. Using this approach, we identified eight pentapeptides, all of which were able to self-assemble into nanoparticles or nanofibers. Some of them were able to interact with and taken up efficiently by HeLa cells. Intracellular distribution varied among these non-toxic peptidic nanoparticles. This novel but very simple screening strategy, has enabled rapid identification of self-assembling peptides suitable for the development of nanostructures for various biomedical and material applications.

Introduction

A total of 20 eukaryotic amino acids allow the creation of tens of thousands of proteins with a stable three-dimensional structure and a variety of functionalities. Although short linear peptides (5-mer to 10-mer) lack a stable three-dimensional structure, some of them may have a stable secondary structure. Others may possess self-assembling properties. It is well documented that the shortest peptides with two amino acids can act as powerful self-assembly motifs[1,2], giving rise to stable material, creating opportunities for rational functional design of novel materials with semiconductivity[3], piezoelectric[4,5], and fluorescence properties[6,7]. To develop these functional materials, both L- and D- amino acids as well as unnatural amino acids can be used. However, for *in vivo* biological applications, eukaryotic L-amino acid containing peptides may be preferable as peptides with these amino acids are inherently biodegradable, making them more biocompatible and may be less toxic.

It is well-known that peptide self-assembly can form a variety of morphological structures, such as nanoparticles[8,9], nanofibers[10-12], nanotubes[1,13,14] and nanosheets[15,16]. The self-assembling process can be attributed from hydrogen bonding, salt bridges, metal chelation, hydrophobic interactions, π−π interactions, and/or van der Waals interactions[17] between the peptide chains. Although there are simple rules for the design of self-assembling peptides, based on known hydrophobic interactions, salt-bridges, and hydrogen bonding between peptide chains in water[18], the rules are empiric and far from meeting the application demands in various fields.

There are three common approaches for the development of self-assembling peptides. 1) Empirical design: most sequence design based on natural assembly peptides from biological systems such as KLVFF derived from parts of amyloid protein $A\beta_{16-20}$[19], and NFGAIL derived from a fragment of human islet amyloid polypeptide[20]. 2) Computational screening: the aqueous self-assembly propensity of

tripeptides and dipeptides, such as PFF, and KYF, and KFD were successfully screened and identified by computational method.[21] 3) Continuous enzymatic condensation induced hydrolysis and sequence exchange based on unprotected homo- and heterodipeptides (based on amino acid F, L, W, S, D), creating a dynamic combinatorial peptide library for the discovery of self-assembling structures with different amino acid sequences and consequent nanoscale morphologies[22]. Nonetheless, there is great need to create a more facile and unbiased tool for the rapid discovery of new self-assembling peptides.

One-bead one-compound (OBOC) combinatorial peptide library method, first described by Lam et al in 1991, has been used extensively in the discovery of ligands against cell surface receptors, target proteins, host molecules for small molecules, protease substrates, kinase substrates, membrane active peptides, small molecule inhibitors against galectin-1[23]. OBOC libraries is not limited to natural amino acids; it offers a lot more structural possibilities, e.g. linear, cyclic, branch and macrocyclic peptide libraries, as well as peptide libraries comprised of both natural and unnatural amino acids (L-/D-, α-/β-/γ-amino acids) and amino acids with post translational modifications such as phosphorylation, glycosylation, methylation, and glycation[24]. It can also be applied to the generation of small molecules, glycopeptides, lipopeptide, peptoid and unnatural foldamers.

We believed the versatile and enabling OBOC combinatorial technology would enable us to develop self-assembling peptides efficiently if we could develop a simple but robust screening method to identify the self-assembled peptides on beads. We rationalized that fluorescent probes responsive to hydrophobic environment will allow us to illuminate hydrophobic pockets formed by self-assembled peptides on the beads. One such fluorescent probe is nitro-1,2,3-benzoxadiazole (NBD), which is known to fluorescent activate under hydrophobic environment. [25] NBD could be added as free dye or tethered to the peptide chain. We elected the latter for our peptide library design (Figure 1).

Results And Discussion

Validation of fluorescent-activation screening assay for self-assembling peptides. It is well known that $A\beta_{16-20}$ peptide sequence KLVFF can self-assemble into nanofibers in water[19]. We therefore chose it as a model peptide to test our screening strategy, and used KAAGG as the non-assembling negative control.[26] These control peptides, N-terminally capped with NBD were synthesized with standard Fmoc-chemistry, and TentaGel S resin beads as solid support but without any cleavable linker. After side-chain deprotection, the beads were thoroughly washed with DMF, which was replaced stepwise with water or methanol and then examined under a fluorescent microscope. In methanol, both (NBD)-KLVFF-beads and (NBD)-KAAGG-beads showed bright fluorescence. This is expected as the hydrophobicity-sensitive fluorescence dye NBD would fluoresce brightly under hydrophobic condition, in this case methanol. In water, we expect fluorescent signal emitted from non-sequestered NBD to diminish, unless it is buried inside a hydrophobic environment such as within peptide aggregates or β-sheets formed by KLVFF peptides. This was exactly what was observed: under aqueous condition, (NBD)-KLVFF-beads fluoresced brightly but (NBD)-KAAGG-beads did not (Figure 2a and S1). Similar to KLVFF, two other peptides

(NFGAIL, LIVGD)[27] with known self-assembling properties were found to yield similar results, and therefore were utilized as two additional positive controls (Figure S2). These results were gratifying as it demonstrated that such a simple assay would allow one to rapidly screen and identify self-assembling peptides from OBOC combinatorial libraries.

Screening of new self-assembling peptides. Once the screening method has been validated with our model KLVFF peptide, a totally random pentapeptide library with 19^5 permutations (cysteine was omitted from the library) was constructed using our previously published methods (Figure S3)[23]. Again, TentaGel S resin (loading of 0.31mmol/g) was used as the solid support. The pentapeptides in the library were N-terminally capped with NBD. Figure 2b shows the screening result of a representative region of a plate containing the OBOC library. The positive beads with an intense fluorescent signal (arrowed) were noted. The rest of the beads were considered negative beads. From a total of 100,000 beads screened, we selected a total of eight strongest fluorescent positive beads and four dark beads as negative beads. These 12 beads were physically isolated for automatic Edman sequencing, and the result is shown in Table 1. The peptides were then resynthesized in soluble form and purified by high performance liquid chromatography HPLC for testing (Figure S4-12). The amino acid sequences of the 8 self-assembling pentapeptides are FTISD, ITSVV, YFTEF, ISDNL, LDFPI, FAGFT, FGFDP and FFVDF. Not unexpectedly, of the 40 amino acids in these 8 pentapeptides, 50% are hydrophobic residues, predominated by Phe (11 Phe, 4 Ile, 3 Val, and 2 Leu). For the remaining 20 amino acids, 6 are acidic residues (5 Asp and 1 Glu) and 7 are neutral and hydrophilic (4 Thr and 3 Ser). The rest are: 2 Pro, 2 Gly, 1 Tyr, 1 Asn, and 1 Ala. All eight peptides have at least two hydrophobic residues. Six out of the 8 peptides have one negatively charged residue (Asp or Glu). The remaining two peptides are neutral. Interestingly even though our model peptide KLVFF has a Lys, none of the 8 identified self-assembling peptides has any basic residue. For the Pro containing pentapeptides, LDFPI and FGFDP, the Pro residue which promote peptide turns, resides at the fourth and fifth positions, but not in the middle. Not unexpectedly, all the four randomly selected negative non-assembling peptides (RITTR, PLVKA, PFTTR, QIMRW) have very different sequences, and contain at least one positive charged amino acid.

To estimate the propensity of the identified peptides to self-assemble, the critical micelle concentrations (CMC) of the 8 positive peptides and 4 negative peptides were determined, and the results are shown in Table 1 and Figure S13,14. The CMC of all the 8 positive peptides were detectable and found to range between 8.4 to 14.4 mM, indicative of propensity for these peptides to self-assemble under aqueous environment. In contrast, none of the four randomly selected negative peptides had a detectable CMC (Figure S14). Hydrophobicity of peptides can be predicted by the value of GRAVY[28] with more negative value for more hydrophilic peptides. The GRAVY values of both the positive and negative assembling peptides are summarized in Table 1. Of the 4 negative assembling peptides, 2 have a negative GRAVY value. For the rest of the peptides, both positive and negative assembling, have GRAVY values ranging from 0.02 to 2.28, indicating that hydrophobicity alone is not a good predictor of self-assembling property. Experimental testing, such as the screening strategy described in this work, is needed. This is because multiple factors, including hydrophobicity, hydrogen-bonding, electrostatic interactions, and

positions of each residue within the peptides, all contribute to the assembling and final morphology of the self-assembled nano-structure.

Table 1. Peptide information screened from OBOC library

Penta-peptide	Fluorescence (beads)	Assembly	CMC (μM)	Charge	GRAVY
FTISD	ON	YES	10.04	-	0.46
ITSVV	ON	YES	14.8	0	2.28
YFTEF	ON	YES	11.4	-	0.02
ISDNL	ON	YES	9.4	-	0.1
LDFPI	ON	YES	8.4	-	1.2
FAGFT	ON	YES	13.9	0	1.26
FGFDP	ON	YES	14.8	-	0.02
FFVDF	ON	YES	14.4	-	1.82
RITWI	OFF	NO		+	0.58
PLVKA	OFF	NO		+	0.86
PFTTR	OFF	NO		+	-0.94
QIMRW	OFF	NO		+	-0.5

Evaluation of assembling structures of pentapeptides. To further characterize these self-assembling peptides, we selected two positive peptides (FFVDF and YFTEF) and a negative control peptide (PFTTR) for the following studies: fourier transform infrared (FT-IR) spectroscopy, UV-vis spectra and transmission electron microscopy (TEM). At 30 mM concentration in water, FFVDF generated a milky white solution, and TEM studies revealed an entangled fibrous network (Figure 3a). YFTEF, dissolved in water at 30 mM was found to form a milky hydrogel, and an entangled fibrous network was observed under TEM (Figure 3b). PFTTR (negative control) dissolved in water at 30 mM, as expected, showed a completely clear solution with no nanostructures observed under TEM (Figure 3c). The results indicated that peptide FFVDF and YFTEF can self-assemble, and suggested that the screening method employed here was reliable for the identification of self-assembling peptides.

Self-assembling peptide amphiphiles are often evaluated with IR spectroscopy through characterization of β-sheets structure, with characteristic “amide I” infrared (IR) absorption bands, which are commonly found in these peptide amphiphiles[29]. For example, due to intermolecular hydrogen bonding involving the amide groups, the 1640^{-1} ~1655 cm^{-1} amide I absorption band of free peptides in solution typically narrows and red-shifts to a lower frequency upon self-assembly. This phenomenon was observed in both FFVDF and YFTEF peptides (Figure 3d), with the amide I absorption significantly narrowed and shifted to 1630 cm^{-1}, corresponding to a β-sheet-like arrangement of the amide groups, compared to the negative non-aggregating peptide PFTTR with absorption at 1641 cm^{-1}, signifying random coil structure. The absorption peaks at 1630 cm^{-1} and 1664 cm^{-1} of YFTEF and FFVDF are consistent with anti-parallel β-sheet structures.

To further confirm the peptide assembling in water, the solutions of pentapeptide were diluted to 20 μM for turbidity test. As shown in Figure 3e, among the 3 peptide solutions tested, FFVDF showed the lowest transmittance in the range of visible light (400-780 nm). The transmittance of FFVDF, YFTEF and PFTTR at 400 nm was determined to be 88%, 98% and 100%, respectively, suggesting that FFVDF and YFTEF did self-assemble in water.

Given that FFVDF exhibited strong propensity to self-assemble in water, it was further characterized with both X-ray power diffraction pattern (Figure 3f), TEM (Figure 3g), and selected-area electron diffraction (SAED) (Figure 3h). The results showed an ordered structure of FFVDF nanofibrils. The observed and calculated-spacings of FFVDF nanofibrils were listed in Table S1. According to the X-ray and electron diffraction data of the nanofibers (Figure 3f and 3h), we deduced that the crystal structure of FFVDF in the nanofibers is orthorhombic with cell parameters of a = 9.5, b = 35.3, and c = 45.6 Å. Based on the above data, we established a packing model with one-unit cell comprised of four dimers by adopting Cerius^2 modeling package. These four dimers oriented at two crossed-direction as displayed in Figure 3i. Each dimer is made up of two strands connected by the hydrogen bonding. The hydrogen-bonding direction is along the c-axis. Strong or weak interface was formed within one dimer or between the neighboring two dimers, respectively, confirming the anti-parallel β-sheet structures.

The interactions between self-assembling peptides and living cells. Self-assembling peptides with good biocompatibility may be used to construct nanocarriers for drug delivery. We recently reported the use of FFVLK, the reverse sequence of KLVFF, as self-aggregating b-sheet forming domain for the delivery of HER2 targeting peptides for successful treatment of breast cancer in xenograft models[30]. Such FFVLK containing peptide is able to self-assemble into nanoparticles. Upon intravenous administration, the FFVLK-nanoparticle was able to transform into nanofibrillar network when encountering HER2 at the tumor sites. To investigate the morphology of the nano-assembly formed by the 8 self-assembling peptides, we dissolved each of these peptides in DMSO (5 mM) and then diluted them 100X with water at a final peptide concentration of 50 μM to induce spontaneous self-assembly. Each sample was fixed immediately after peptide solution preparation and at 4 h time point for subsequent TEM processing and analysis. As clearly shown in Figure 4a, all 8 self-assembling peptides initially formed some nanostructures: nanoparticles for ITSVV, YFTEF, ISDNL, LDFPI, FAGFT, FGFDP, and FTISD; nanofibers for FFVDF. Some of the nanoparticles were found to evolve over the 4 h time period to a larger size including FTISD, ITSVV, YFTEF, ISDNL, FAGFT and FGFDP. In addition, 31 nm ITSVV nanoparticles were found to enlarge 10-times to a size of ~300 nm after 4 h. LDFPI (8 nm) maintained the particulate morphology without changing of diameter in 4 h. FFVDF formed nanofibers at 0 and 4 h. After 24 h, all the eight pentapeptides were found to transform to fibrils (Figure S15). These fibrils were then subjected to thermal annealing at 90 °C for 5 h, after which no significant change in morphology was observed under TEM (Figure S16), indicating that these peptide fibrils were at the thermodynamic minimum state. Time-dependent size variations of pentapeptides in water were further confirmed by DLS spectra (Figure S17). The initial diameters of nanoparticles formed by 7 pentapeptides were larger than that observed by TEM, probably due to hydration radius. Size of nanostructure increased over time, correlating well with the

morphologic transformation. In contrast to the self-assembling peptides, no nanostructures were detected in any of the negative control PFTTR, RITWI, PLVKA and QIMRW peptide preparations (Figure S18), which is consistent with the CMC results. Circular dichroism (CD) was used to monitor the secondary structures of the nano-assembly of the eight self-assembling peptides over time (Figure S19). Seven of the eight pentapeptides, except for FFVDF, showed stable CD spectra over 72 h, indicating no changes in secondary structures during the morphological transformation. FFVDF, on the other hand, exhibited weaker cotton effect peaks in 72 h, indicating a decrease of chirality in FFVDF assemblies.

Finally, we examined the biological effects and cellular distribution of the 8 self-assembling peptides on HeLa cells. CCK-8 cell viability assay results suggested that 8 self-assembling peptides were non-toxic to HeLa cells up to a concentration of 200 μM (Figure S20). In order to observe the nanomaterials under fluorescent microscopy, each peptide preparation was spiked with 3% of the same peptide N-terminally labeled with FITC, and then added to HeLa cells at a final concentration 40 μM. Our assumption was that FITC decorating 3% of the peptides would not significantly affect the nanostructure, cell uptake and intracellular distribution. After 4 h of incubation with the peptide assemblies, the cells were observed under a fluorescent microscope (Figure 4c, 4d and S21). Obvious cellular uptake was observed in 5 of the 8 peptides (YFTEF, ISDNL, LDFPI, FAGFT, and FGFDP). It is clear that LDFPI nanoparticles were able to permeate the cells and eventually localized to the nucleus and perinuclear areas (Figure 4d). It is important to note that LDFPI nanoparticle was small (8 nm diameter) even after 4 h incubation. Its small size may in part explain its ability to pass through the nuclear pore complexes[31,32]. YFTEF nanoparticles (41 nm evolved to 75 nm after 4 h) were found to be distributed throughout the cytoplasm but not the nucleus; both granular and diffuse staining were observed (Figure S21). ISDNL and FGFDP nanoparticles, both around 30 nm, appeared to distribute only to the cytoplasm, in granular forms. For ISDNL, the FITC green signal was found to co-localize with the Lyso-Tracker red signal, indicating that the nanoparticles were inside the lysozomes. FAGFT nanoparticle was small (10 nm evolved to 15 nm after 4 h) and appeared to mainly confine to the cytoplasm as well (Figure S21). FFVDF formed nanofibers at the outset and formed some fluorescent aggregates outside the cells (Figure 4e). ITSVV, forming ~30-nm nanoparticles at 0 h, with 10-times size increase in 4 h, resulted in staining of the cell membrane and minor staining of the cytoplasm (Figure 4b and S21). FTISD, with size increase over time, stained both the cell membrane and cytoplasm (Figure S21). To evaluate the cell uptake mechanism of peptide assemblies (YFTEF, ISDNL and FGFDP) into the cytoplasm, we treated the cells at 4 °C or with various endocytosis inhibitors (Figure S22). Based on the result of this study, we have determined that endocytic uptake of YFTEF was clathrin dependent; uptake of ISDNL was through caveolae-dependent endocytosis and micropinocytosis; FGFDP uptake was both caveolae-dependent and clathrin-dependent. Although all three peptide assemblies (YFTEF, ISDNL, and FGFDP) ended up in lysosome (Figure 4c & Figure S23), their intracellular trafficking kinetics were found to be different. Through time-dependent fluorescence co-localization studies with dye-staining lysosome and FITC-labeled peptides (Figure S23), we have found that YFTEF remained in lysosomes for 8 h without obvious escape. In contrast, both ISDNL and FGFDP were found to escape from lysosomes in approximately 4 h and 1.5 h, respectively.

Conclusion

The time-tested one-bead one-compound (OBOC) concept[23] has been applied by many investigators around the world to discover peptide, peptoid, peptidomimetic, and small molecule ligands, enzyme substrates or bioactive molecules in a highly efficient manner. The enabling high-throughput OBOC technology integrates seamlessly the synthesis, screening and decoding steps. Many OBOC screening assays such as protein binding assays, cell-based binding assays and cell-based functional assays have been developed.[24] Here, we report the development of a unique but very simple fluorescent-activation screening method, that has allowed us to rapidly discover self-assembling short peptides for nanomaterial development. Nitro-1,2,3-benzoxadiazole (NBD) placed at the N-terminus of a random penta-peptide library will fluoresce when the displayed peptides self-assemble to form hydrophobic pockets that interact with NBD; free dyes may be also used for screening self-assembly peptides (Figure S24). This proof of concept report validates that the method works well and provides a new tool, not only to discover biological useful nanomaterial, but also allows us to identify novel peptide motifs for self-assembling, in a non-bias manner. As increasing number of peptides are identified with this approach, we may be able to better understand how peptides self-assemble. Although the focus of this report is on self-assembling of the same peptide, we can easily design OBOC libraries for the discovery of hybrid nanomaterial formed by self-assembly of two or more different peptides. Because OBOC libraries are produced by chemical synthesis, the discovered self-assembled nanomaterials are not limited to canonical amino acids. Various nanomaterials with a huge range of building blocks can be developed. The screening process is very simple and can be easily automated. Physicochemical conditions such as pH, ionic strength, solvents, temperature, electric current, and magnetic field can also be incorporated into the screening steps. Sequential screening of immobilized OBOC library-beads[33] under various conditions, in conjunction with optical spectral analysis will enable us to discover novel nanomaterial with desirable properties, including stimuli-responsive property that is very important in biomedical applications.

All eight positive pentapeptides identified in this study was found to be non-toxic to HeLa cells up to at least 200 mM concentration, and have the capacity to self-assemble to form either nanoparticles or nanofibers. Several of these peptidic nanostructures were found to interact with living mammalian cells, either through cell surface binding, or enter cells into the lysosomes, cytoplasm or inside the nucleus. Work is currently underway to use some of these peptides for drug and nucleic acid delivery. As more self-assembling peptides with various unique properties are discovered, we may be able to combine them to make novel nanomaterials for various biomedical applications.

Method

Materials

TentaGel Resin was from Rapp Polymere (Germany, loading 0.31 mmol/g). 9-Fluorenylmethoxycarbonyl (Fmoc)-protected amino acids, 2-(1H-benzotriazole-1-yl)-1,1,3,3-tetramethyluronium hexafluoro-phosphate (HBTU) and Wang resin were obtained from GL Biochem (China). Trifluoroacetic acid (TFA), fluorescein

isothiocyanate (FITC), N-methyl morpholine (NMM), piperidine and N,N'-dimethylformamide (DMF) were all from Beijing Chemical Plant (China). 1,2-Ethanedithiol (EDT) was purchased from Alfa Aesar (USA). Dimethyl sulfoxide (DMSO) was purchased from Aldrich Chemical Co. and used without further purification. Cyanogen bromide (CNBr) was from J&K Chemical (China). The Hela cell lines were received from the Cell Culture Center of the Institute of Basic Medical Sciences, Chinese Academy of Medical Sciences (Beijing, China). Cell culture medium and fetal bovine serum were from WisentInc (Multicell, WisentInc, St. Bruno. The cell counting kit-8 assay (CCK-8) (Beyotime Institute of Biotechnology, China) was used. Hela cells were maintained Dulbecco's Modified Eagle's Medium (DMEM) with 10% fetal bovine serum and 1% penicillin. All cells were cultured in a humidified atmosphere containing 5% CO_2 at 37 °C.

The construction and synthesis of OBOC libraries with fluorescence probe NBD

The OBOC pentapeptide libraries (19^5) were built using Fmoc strategy SPPS (solid phase peptide synthesis) (Figure S3). Tentagel Resin ((named N-beads with loading 0.31 mmol/g) were separately used as the solid phase support. The pentapeptide sequence of X_1 X_2 X_3 X_4 X_5 were constructed in the libraries, in which $X_1 \sim X_5$ represents either Ala, Asp, Glu, Phe, Gly, His, Ile, Lys, Leu, Met, Asn, Pro, Gln, Arg, Ser, Thr, Val, Trp, Tyr residues. During the synthesis of OBOC library, solid support beads were mixed and split equally in each cycle, then different amino acids were added, separately[23], the process were repeated 4 times. The synthesis of peptides was used dehydrous DMF as solvent. The Fmoc group was removed by 20% (v/v) piperidine in DMF and the deprotection time was 10 min each times. During the coupling step, the HBTU (4 mM) and Fmoc-amino acid (4 mM) were dissolved in DMF containing NMM (0.4 mM). The coupling time was 50 min. Qualitative Fmoc deprotection and coupling were confirmed by ninhydrin test (ninhydrin, phenol, VC 1:1:1 v/v). All the above experiments were carried out in the solid phase peptide synthesis vessels with sieves in it. After pentapeptides libraries were built, the beads were swollen in water for 24 h, outer layer reacted with Fmoc-OSu and inner core reacted with $(Boc)_2O$. After Fmoc-deprotection of the outer layer, NBD-COOH was conjugated to the N-terminus of the library peptide.[34] The bilayer bead pentapeptide library was ready for screening for self-assembling peptide after deprotection with a cocktail of cleavage reagents (95%, TFA: 2.5% water: 2.5% EDT v/v).

Synthesis of pentapeptides

Positive and negative peptides by self-assembly screening process were de novo synthesized by solid-phase methods using a standard Fmoc-Chemistry. Wang Resin was used as the solid phase support. The synthesis process was basically consistent with above peptide synthesis. After elongation, cleavage reagents (95%, TFA: 2.5% water: 2.5% EDT v/v) were used for cleaving the peptide chain from beads for 3 h. The TFA was removed by evaporating by vacuum rotary to obtain concentrate product. Then the product was precipitated in cold anhydrous diethyl ether, centrifuged, dried to obtain the crude peptides. The peptides were purified by preparative reversed-phase high performance liquid chromatography (HPLC) with a preparative reversed-phase Inertsil C18 HPLC column (ODS-3, 5 μm, 20 ×250 mm). A linear gradient of acetonitrile/water with 0.1% TFA respectively from 5/95 (v/v) to 70/30 (v/v) during 18 min, then 70/30 (v/v) to 90/10 (v/v) in 4 min and in this flow continue 1 min ,next return to 5%/95%(v/v) tilled

for 3 min was used as the mobile phase. The separation was performed with a flow rate of 1 mL/min and the monitoring wavelength was 220 nm using a UV detector (Waters 2535Q). The purified peptides were determined matrix-assisted laser desorption ionization time-of-flight mass spectrometry (MALDI-TOF-MS, Bruker Daltonics, USA) and liquid chromatography-mass spectrometry (LC-MS 8050, Shimadzu, Japan).

Preparation of peptide-based nanomaterials

Pentapeptides monomers were dissolved in DMSO at a concentration of 5.0 mM, followed by quick injection into water at a volume ratio of 1:99 for DMSO and H_2O to obtain the nanomaterials solution (50 μM). For 30 mM pentapeptide solution, the pentapeptide was dissolved in water and sonicated for 3 min.

Transmission Electron Microscopy (TEM) for the morphology

The pentapeptide solution with the concentration of 20 μM (10 μL) were placed dropwisely onto a copper mesh for 5 min, then most of the liquid was removed through a filter paper. Ten microliters of uranyl acetate solution was employed to stain the samples for 5 min, followed by drying the spare liquid with the filter. Finally, the copper mesh was washed with 10 μL of deionised water, which was blotted after staining and drying at room temperature. All of the samples were observed by TEM (Tecnai G2 20 S-TWIN) at an accelerating voltage of 200 kV.

TEM and Selected Area Electron Diffraction (SAED)

We use JEOL-1400 to capture BF image of FFVDF nanofibrils at 110 kV. A selected-area aperture was inserted with an electron diffraction mode. A water droplet containing the nanofibrils was cast onto copper grids with the supporting film.

FT-IR spectra

The pentapeptide with a concentration of 20 μM were freshly prepared. The solution was used for FT-IR measurement. The solution mentioned above lyophilised to obtain the powders for XRD measurements. The FT-IR spectrum was recorded on a spectrometer (Spectrum One, Perkin Elmer Instruments Co., Ltd.). The XRD spectrum was recorded on a Xeuss SAXS/WAXS system (Xenocs Asia Pacific Pte., Ltd.).

CD Spectra

The CD spectra of pentapeptides (40 μM) were collected at room temperature using a CD spectrometer (JASCO-1500, Tokyo, Japan) with a cell path length of 1 mm. The measurements were implemented between 190 nm and 230 nm with a resolution of 1.0 nm and a scanning speed of 300 nm/min. For each measurement, 3 spectra were collected and averaged.

CLSM observation

Hela cells cultured with and pentapeptide nanomaterials (50 μM) were imaged using a Zeiss LSM710 confocal laser scanning microscope (Jena, Germany). The Hela cells were seeded in complete DMEM in a

humidified atmosphere with 5% CO_2 and then cultured at 37 °C overnight. Then, 1 mL of serum-free fresh medium containing pentapeptide (50 μM) was used for replacing the medium, and the cells were cultured for 4 h and washed with PBS three times before being imaged using a Zeiss LSM710 confocal laser scanning microscope with a 40× objective lens.

Statistical analysis

All data are reported as the mean ± standard deviation (s.d.). The in vitro experiments were performed in three independent experiments with at least three technical replicates.

Declarations

Funding: This work was supported by the National Natural Science Foundation of China (51890891, 51890894, 51725302, 21807020, 51573031 and 51573032), Science Fund for Creative Research Groups of the National Natural Science Foundation of China (11621505).

Author contributions: L. W., R.W. L., and K.S. L. conceived the project. P.P. Y., Y.J. L., L. W., H. W., R.W. L., and K.S. L. planned and designed the experiments. P.P. Y., Y.J. L. L. W. and R.W. L. performed most of the experiments. Y. C. and Z.W. L. performed the structural analysis. L. Z. assisted with the chemical synthesis, and K. Z., W.W. X., and H. C., assisted with the cell culture studies. J.Q. W. assisted the experiments in revision. P.P. Y., Y.J. L., and Y. C. contributed equally to this work.

Competing interests: The authors filed patents pertaining to the results presented in the paper. The authors declare the following competing financial interest(s): L. W. H. W., P.P. Y. and Y.J. L. are the co-inventors of a pending patent. The remaining authors declare that they have no competing interests.

Data and materials availability: All data needed to evaluate the conclusions in the paper are present in the paper and/or the Supplementary Materials. Additional data related to this paper may be requested from the authors.

References

1 Reches, M. & Gazit, E. Casting Metal Nanowires within Discrete Self-Assembled Peptide Nanotubes. *Science* **300**, 625-627 (2003).

2 Liu, K. *et al.* Simple Peptide-Tuned Self-Assembly of Photosensitizers towards Anticancer Photodynamic Therapy. *Angew. Chem. Int. Edit.* **55**, 3036-3039 (2016).

3 Tao, K., Makam, P., Aizen, R. & Gazit, E. Self-Assembling Peptide Semiconductors. *Science* **358** (2017).

4 Kholkin, A. *et al.* Strong Piezoelectricity in Bioinspired Peptide Nanotubes. *ACS Nano* **4**, 610-614 (2010).

5 Vu, N., Zhu, R., Jenkins, K. & Yang, R. Self-Assembly of Diphenylalanine Peptide with Controlled Polarization for Power Generation. *Nat. Commun.* **7** (2016).

6 Fan, Z. *et al.* Near Infrared Fluorescent Peptide Nanoparticles for Enhancing Esophageal Cancer Therapeutic Efficacy. *Nat. Commun.* **9**, 2605 (2018).

7 Burggraaf, J. *et al.* Detection Of Colorectal Polyps in Humans Using an Intravenously Administered Fluorescent Peptide Targeted Against c-Met. *Nat. Med.* **21**, 955-961 (2015).

8 Liu, L. *et al.* Self-Assembled Cationic Peptide Nanoparticles as an Efficient Antimicrobial Agent. *Nat. Nanotechnol.* **4**, 457-463 (2009).

9 MacKay, J. A. *et al.* Self-Assembling Chimeric Polypeptide-Doxorubicin Conjugate Nanoparticles That Abolish Tumours after a Single Injection. *Nat. Mater.* **8**, 993-999 (2009).

10 Aida, T., Meijer, E. W. & Stupp, S. I. Functional Supramolecular Polymers. *Science* **335**, 813-817 (2012).

11 Gazit, E. Self-Assembled Peptide Nanostructures: the Design of Molecular Building Blocks and Their Technological Utilization. *Chem. Soc. Rev.* **36**, 1263-1269 (2007).

12 Webber, M. J., Appel, E. A., Meijer, E. W. & Langer, R. Supramolecular Biomaterials. *Nat. Mater.* **15**, 13-26 (2016).

13 Ghadiri, M. R., Granja, J. R. & Buehler, L. K. Artificial Transmembrane Ion Channels from Self-Assembling Peptide Nanotubes. *Nature* **369**, 301-304 (1994).

14 Gao, X. Y. & Matsui, H. Peptide-Based Nanotubes and Their Applications in Bionanotechnology. *Adv. Mater.* **17**, 2037-2050 (2005).

15 Dai, B. *et al.* Tunable Assembly of Amyloid-Forming Peptides into Nanosheets As a Retrovirus Carrier. *P. Natl. Acad. Sci. USA* **112**, 2996-3001 (2015).

16 Sanii, B. *et al.* Shaken, Not Stirred: Collapsing a Peptoid Monolayer To Produce Free-Floating, Stable Nanosheets. *J. Am. Chem. Soc.* **133**, 20808-20815 (2011).

17 Cui, H., Webber, M. J. & Stupp, S. I. Self-Assembly of Peptide Amphiphiles: From Molecules to Nanostructures to Biomaterials. *Biopolymers* **94**, 1-18 (2010).

18 Ma, M. *et al.* Aromatic-Aromatic Interactions Induce the Self-Assembly of Pentapeptidic Derivatives in Water To Form Nanofibers and Supramolecular Hydrogels. *J. Am. Chem. Soc.* **132**, 2719-2728 (2010).

19 Tjernberg, L. O. *et al.* Arrest of beta-amyloid fibril formation by a pentapeptide ligand. *J. Biol. Chem.* **271**, 8545-8548 (1996).

20 Azriel, R. & Gazit, E. Analysis of the Structural and Functional Elements of the Minimal Active Fragment of Islet Amyloid Polypeptide (IAPP) - an Experimental Support for the Key Role of the Phenylalanine Residue in Amyloid Formation. *J. Biol. Chem.* **276**, 34156-34161 (2001).

21 Frederix, P. W. J. M. *et al.* Exploring the Sequence Space for (Tri-) Peptide Self-Assembly to Design and Discover. *Nat. Chem.* **7**, 30-37 (2015).

22 Pappas, C. G. *et al.* Dynamic Peptide Libraries for the Discovery of Supramolecular Nanomaterials. *Nat. Nanotechnol.* **11**, 960-967 (2016).

23 Lam, K. S. *et al.* A New Type of Synthetic Peptide Library for Identifying Ligand-Binding Activity. *Nature* **354**, 82-84 (1991).

24 Liu, R., Li, X., Xiao, W. & Lam, K. S. Tumor-Targeting Peptides from Combinatorial Libraries. *Adv. Drug Deliv. Rev.* **110**, 13-37 (2017).

25 Kuerschner, L. *et al.* Polyene-Lipids: a New Tool to Image Lipids. *Nat. Methods* **2**, 39-45 (2005).

26 Yang, P.-P. *et al.* Reorganization of Self-Assembled Supramolecular Materials Controlled by Hydrogen Bonding and Hydrophilic-Lipophilic Balance. *J. Mater. Chem. B* **4**, 2662-2668 (2016).

27 Hauser, C. A. E. *et al*. Natural tri- to hexapeptides self-assemble in water to amyloid β-type fiber aggregates by unexpected α-helical intermediate structures. *Proc. Natl. Acad. Sci.* **108**, 1361 LP – 1366 (2011).

28 Goshe, M. B., Blonder, J. & Smith, R. D. Affinity Labeling of Highly Hydrophobic Integral Membrane Proteins for Proteome-Wide Analysis. *J. Proteome. Res.* **2**, 153-161 (2003).

29 Fleming, S. *et al.* Assessing the Utility of Infrared Spectroscopy as a Structural Diagnostic Tool for β-Sheets in Self-Assembling Aromatic Peptide Amphiphiles. *Langmuir* **29**, 9510-9515 (2013).

30 Zhang, L. *et al.* Transformable Peptide Nanoparticles Arrest HER2 Signalling and Cause Cancer Cell Death In Vivo. *Nat. Nanotechnol.* **15**, 145–153(2020).

31 Kubitscheck, U. *et al.* Nuclear Transport of Single Molecules: Dwell Times at The Nuclear Pore Complex. *J. Cell Biol.* **168**, 233-243 (2005).

32 Meinema, A. C. *et al.* Long Unfolded Linkers Facilitate Membrane Protein Import Through the Nuclear Pore Complex. *Science* **333**, 90-93 (2011).

33 Carney, R. P. *et al*. Combinatorial Library Screening with Liposomes for Discovery of Membrane Active Peptides. *ACS Comb. Sci.*, **19**, 299-307 (2017).

34 Liu, R., Marik, J. & Lam K. S. A Novel Peptide-Based Encoding System for “One-Bead One-Compound” Peptidomimetic and Small Molecule Combinatorial Libraries. *J. Am. Chem. Soc.*, **26**, 7678–

7680 (2002).

Figures

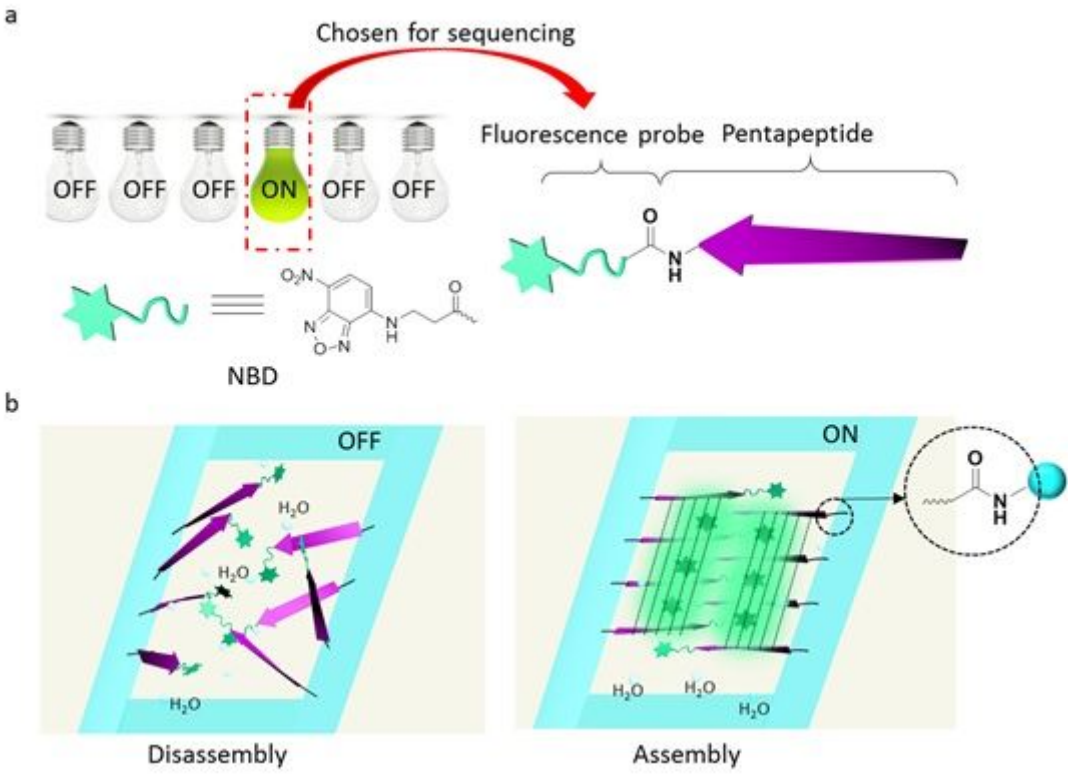

Figure 1

The principle for screening self-assembled peptides based on one-bead one-compound (OBOC) combinatorial peptide library. Self-assembling peptide forms beta-sheet under aqueous condition, creating hydrophobic pockets for fluorescent activation of N-terminally tethered organic dye nitro-1,2,3-benzoxadiazole. The blue band represents the bead matrix of crosslinked polystyrene.

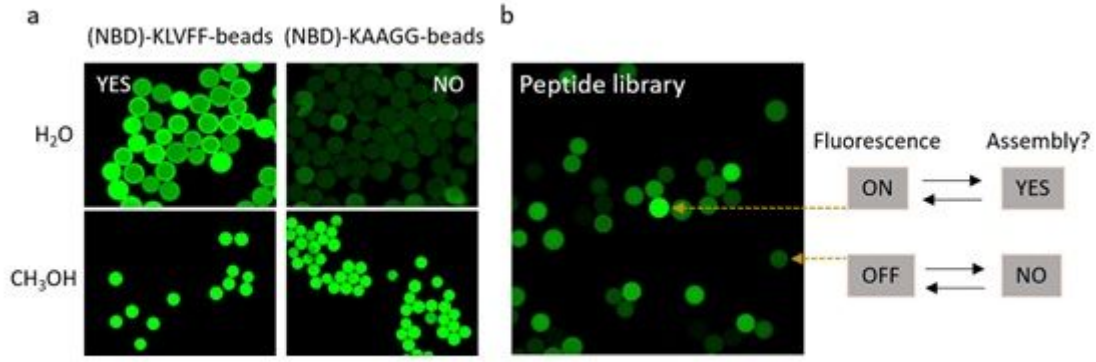

Figure 2

Screening assay development and OBOC library screening for self-assembling peptides. a) The fluorescence microscope imaging of positive control (NBD)-KLVFF-beads and negative control (NBD)-KAAGG-beads in water and methanol after incubation for 20 min. b) Screening result of a representative region of a plate containing the OBOC library. The positive beads with an intense fluorescent signal were detected (arrowed), the remaining beads were negative or weakly fluorescent.

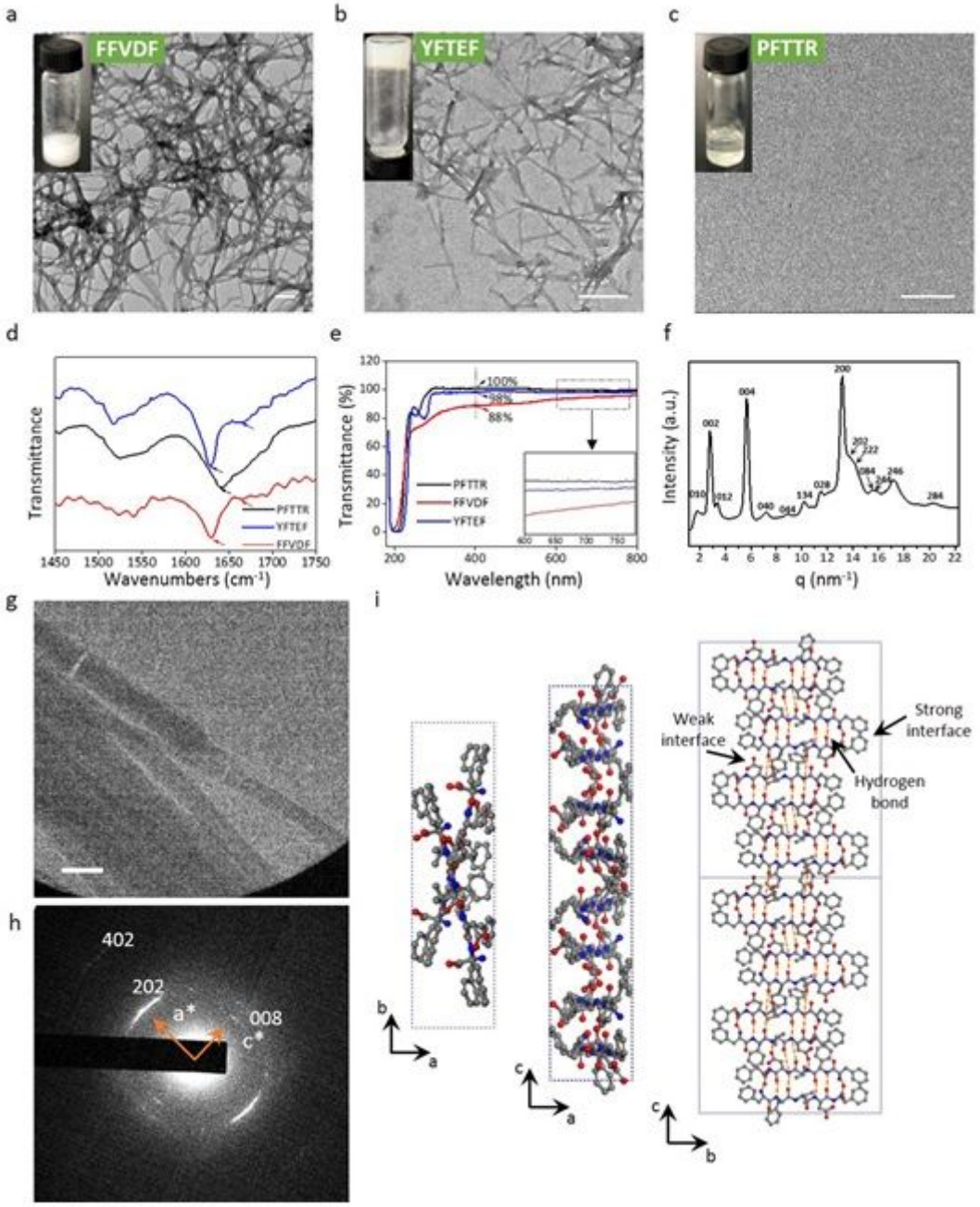

Figure 3

Structural characterization of identified self-assembling pentapeptides. a-c) TEM images of FFVDF, YFTEF and PFTTR pentapeptides (30 mM in H2O). Insets: photographs of the suspension, gel, and solution. d) FT-IR absorption spectra in the amide I region of pentapeptides FFVDF, YFTEF and PFTTR (30 mM in H2O); narrowing and red-shifting of the amide modes of FFVDF and YFTEF indicate the presence

of well-ordered assemblies for these peptides. e) The transmittance spectra of FFVDF, YFTEF and PFTTR at concentration of 20 μM. f) X-ray diffraction powder pattern of FFVDF nanofibrils. g) Bright-field TEM image of nanofibrils self-assembled from FFVDF (30 μM in H2O with 1% DMSO). h) Selected-area electron diffraction (SAED) pattern of the nanofibers corresponding to the part of BF image in h. i) ab-, ac-, bc-plane projections of the proposed molecular packing model of the nanofibers based on SAED and powder X-ray diffraction results. The scale bar is 200 nm

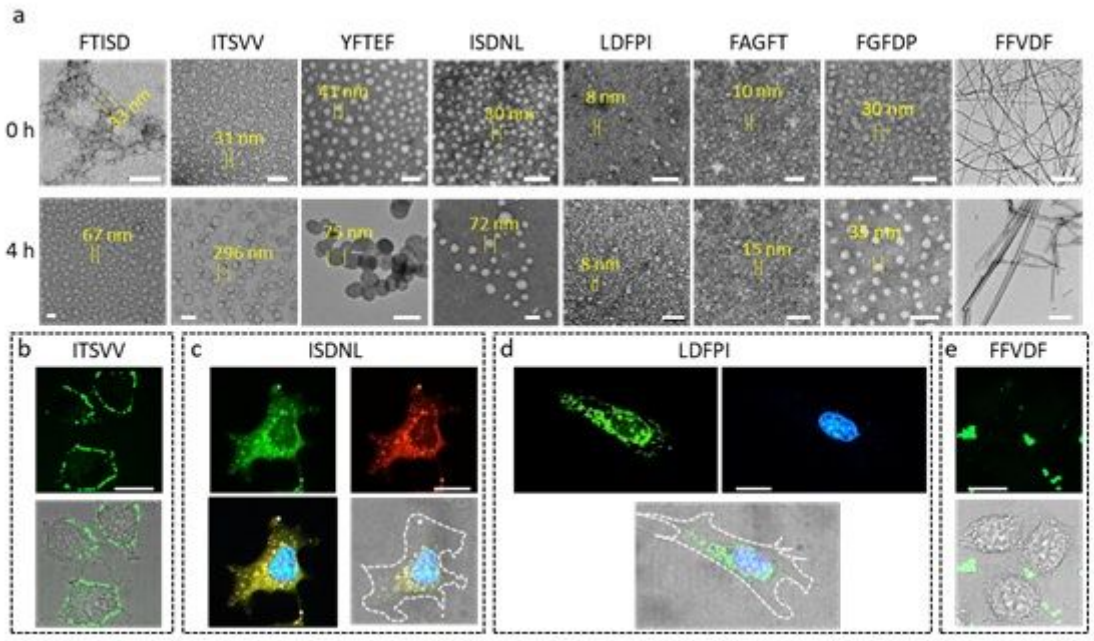

Figure 4

a) Structure transformation and cellular distribution of pentapeptide-based nanomaterials. TEM images of 40 μM chemically synthesized FTISD, ITSVV, YFTEF, ISDNL, LDFPI, FAGFT, FGFDP and FFVDF “solubilized” in H2O with 1% DMSO for 0 and 4 h. The scale bar is 100 nm for FTISD, YFTEF, ISDNL, LDFPI, FAGFT and FGFDP at both 0 h and 4 h, and ITSVV at 0 h. The scale bar is 500 nm for FFVDF at both 0 h and 4 h and ITSVV at 4 h. b-e) Pentapeptide assemblies (40 μM) interaction with live HeLa cells. ITSVV (b) localized on the cell membrane, ISDNL (c) distributed inside the lysosomes throughout the cytoplasm, LDFPI (d) localized to the nucleus and perinuclear areas, and FFVDF (e) formed aggregates outside the cell. Green denotes FITC-labeled pentapeptides. Red (Lyso-Tracker Red) denotes lysosomes, Blue (Hoechst 33324) is nucleus. The scale bar is 20 μm. The dash line outlines the cell membrane.

Supplementary Files

This is a list of supplementary files associated with this preprint. Click to download.

- SupplementaryMaterials.pdf